ISSN 1533-9211

DOI: 10.5281/zenodo.21867143

COMPARATIVE ANALYSIS OF CELLULAR RADIO WAVE PATHLOSS IN URBAN SUB-URBAN AND RURAL ENVIRONMENTS

AMIR DENTI[1], GUNAWAN[2], ARIEF MARDIANTO[3], FAKH RUR RAZI[4], HANAFI[5] and INDRAWATI[6]*

[1,2,3,4,5]Electro Engineering Department, Polytechnic State Lhokseumawe, Aceh, Indonesia.
[6]Information Technology and Computer Department, Polytechnic State Lhokseumawe, Aceh, Indonesia.
*Corresponding Author Email: indrawati@pnl.ac.id

Abstract

Accurate path loss characterization is essential for wireless network design and optimization. This study compares radio wave path loss in urban, suburban, and rural environments based on field measurements at 1870 *MHz* in Lhokseumawe, Indonesia. The Log-Distance Path Loss model was used to estimate the path loss exponent and average path loss. Results show that received power decreased and path loss increased with distance. Average path loss values were 103.897 *dB*, 146.791 *dB*, and 155.589 *dB* for urban, suburban, and rural environments, respectively. The findings highlight the importance of site-specific measurements for accurate propagation modeling and wireless network planning.

Keywords: Radio Wave Propagation, Path Loss, Log-Distance Path Loss Model, Urban, Suburban, Rural.

1. INTRODUCTION

The improvement in housing quality has accelerated the growth and development of residential areas, leading to the construction of high-rise buildings and commercial facilities in urban, suburban, and rural environments [1]. These environmental changes significantly affect radio wave propagation between the transmitter (T_x) and receiver (R_x), as the propagation environment strongly influences signal transmission characteristics [2], [3]. During propagation, radio waves interact with surrounding objects through reflection, diffraction, scattering, penetration, and absorption. These propagation mechanisms alter the signal path and increase the effective propagation distance, resulting in signal attenuation commonly referred to as path loss [3]–[5].

Previous studies have extensively investigated the effects of atmospheric factors, such as temperature, humidity, and air pressure, on radio wave propagation [6], [7]. In contrast, this study focuses on the influence of surrounding physical objects on signal propagation. Various propagation models have been developed to estimate path loss under different environmental conditions, including empirical, deterministic, and theoretical models [8], [9]. To evaluate the impact of environmental characteristics, three representative propagation environments—urban, suburban, and rural—were selected, as these are widely used in large-scale wireless propagation studies [10]. This study presents a comparative analysis of radio wave path loss in urban, suburban, and rural environments using the Telkomsel 4G LTE network in Lhokseumawe, Indonesia. Path loss was estimated using the Log-Distance Path Loss model, which predicts the average received signal power as a function of propagation distance and

ISSN 1533-9211

DOI: 10.5281/zenodo.21867143

environmental characteristics. This model is widely adopted for large-scale propagation analysis because it effectively characterizes signal attenuation under varying terrain and clutter conditions [11], [12].

Propagation performance was evaluated using the Reference Signal Received Power (RSRP), the primary LTE metric for assessing downlink coverage and signal propagation quality [13], [14]. RSRP measurements were collected at multiple observation points along the propagation path, where the measurement distances were defined as multiples of the far-field reference distance (d_o). Field measurements were conducted using the drive-test method with the Network Cell Info Lite application installed on an Android smartphone. This approach has been widely employed in recent studies to evaluate LTE network coverage, signal quality, and radio propagation performance under real deployment conditions [15], [16].

Three representative measurement sites were selected to reflect different propagation environments. Jalan Merdeka, Lhokseumawe, represents an urban environment characterized by dense buildings and commercial activities. Gampong Beunot, Syamtalira Bayu, represents a suburban environment with moderate building density and vegetation. Gang Payah Jaloh, Jalan Pipa, Punteut, Lhokseumawe, represents a rural environment dominated by open areas, vegetation, and sparse infrastructure. These sites were selected to investigate the influence of environmental characteristics on radio wave propagation and path loss under practical 4G LTE deployment conditions.

2. MATERIAL AND METHOD

Setup Measurement

Previous studies have extensively investigated radio wave path loss in urban, suburban, and rural propagation environments through empirical field measurements and drive-test campaigns. Building on these studies, this work employs the Log-Distance Path Loss model to characterize large-scale radio wave propagation by integrating field measurement data with analytical modeling.

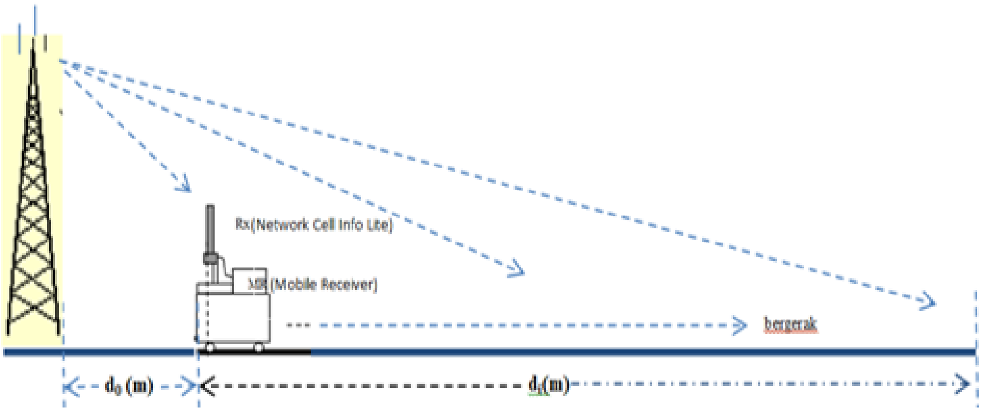

Figure 1: Method for Measuring the Power of Radio Waves Reaching the Receiver

ISSN 1533-9211
DOI: 10.5281/zenodo.21867143

This approach enables a comprehensive characterization of signal attenuation under different propagation environments and provides a reliable basis for comparing path loss characteristics across diverse terrain conditions. The overall measurement procedure adopted in this study is illustrated in Fig. 1.

Field measurements were conducted by recording variations in the received signal power along the propagation path between the transmitter T_x and the receiver R_x. The measurement campaign began at the reference distance, d_0, and continued to successive observation points, d_i, where $d_i > d_0$, to ensure that all measurements were performed within the far-field region required by the Log-Distance Path Loss model [17], [18].

The far-field region of the transmitting antenna is defined as the region beyond the antenna's near-field boundary, where the radiated electromagnetic waves exhibit stable propagation characteristics. This region is determined by the largest linear dimension of the transmitting antenna and the carrier wavelength. The far-field distance is expressed as follows:

$$d_f = \frac{D^2}{\lambda} \tag{1}$$

where D is the largest physical linear dimension of the transmitting antenna. To ensure that the receiver is located within the far-field region, the transmitter-receiver separation distance, $d_0 >$ d, must be greater than the far-field distance, d_f. To be in the far-field region, d_f must satisfy the following condition [19]:

$$d_f \gg \lambda \tag{2}$$

The receiver was positioned at a height of 1.6 m above ground level, representing the typical height of a handheld user device during normal operation. Field measurements were conducted along the propagation path between the transmitter (Tx) and the receiver (Rx). Measurement data were collected at regular observation points with separation distances greater than the carrier wavelength $\lambda(m)$ along the drive-test route to capture the spatial variation in received signal strength (RSS) under different propagation conditions. This measurement configuration is widely adopted in LTE radio propagation studies because it provides reliable large-scale propagation data while minimizing the effects of small-scale fading through spatial averaging [20]–[23].

Log-Distance Path Loss Model

Large-scale radio propagation describes the average attenuation experienced by electromagnetic waves as they propagate from the transmitter (T_x) to the receiver (R_x). One of the most widely used empirical propagation models for terrestrial wireless communication systems is the Log-Distance Path Loss model, which predicts the average received signal power as a logarithmic function of the transmitter–receiver (T_x–R_x) separation distance. Because of its simplicity, computational efficiency, and reliable prediction accuracy, this model has been extensively employed to characterize radio wave propagation in LTE, 4G, and 5G cellular networks under a wide range of propagation environments [24]–[27]. Accordingly, the received

The Seybold Report
ISSN 1533-9211
DOI: 10.5281/zenodo.21867143

signal power at a distance (d) can be expressed as:

$$P_r(d) = P_r(d_0) - 10n\log_{10}\left(\frac{d}{d_0}\right) \quad (3)$$

Where:

$$P_r(d_0) = P_t - PL(d_0) \quad (4)$$

Where $P_r(d)$ is the received signal power (*dBm*) at a distance (d), $P_r(d_0)$ is the received signal power measured at the reference distance (d_0), P_t is the transmitted power, and $PL(d_0)$ is the path loss at the reference distance. The parameter n is the path loss exponent, which characterizes the rate at which the received signal power decreases with increasing propagation distance and reflects the attenuation characteristics of the propagation environment. The corresponding average path loss is expressed as

$$\overline{PL}(dB) = PL(d_0) + 10n\log_{10}\left(\frac{d}{d_0}\right) \quad (5)$$

or equivalently

$$PL(dB) = P_t - P_r(d_0) \quad (6)$$

Where $\overline{PL}(dB)$ is the path loss average (*dB*) at a distance d, $PL(d_0)$ is the path loss (dB) at the reference distance (d_0), (d_0) is the reference distance, and d is the transmitter–receiver T_x–R_x separation distance. These equations indicate that the average received signal power decreases logarithmically as the propagation distance increases. Although the Log-Distance Path Loss model does not explicitly account for multipath fading or shadowing effects, it provides an accurate representation of the average large-scale propagation characteristics in practical wireless environments [28], [29].

Path Loss Exponent

The path loss exponent n is the primary parameter of the Log-Distance Path Loss model because it characterizes the propagation characteristics of a specific environment. Physically, n represents the rate at which the received signal power decreases as the propagation distance increases. In free-space propagation, electromagnetic waves experience only geometric spreading, resulting in a theoretical path loss exponent of $n = 2$. In practical propagation environments, however, additional mechanisms such as reflection, diffraction, scattering, vegetation, and buildings increase signal attenuation, resulting in higher values of n [30]–[32]. Typical path loss exponent values reported in the literature are summarized in Table I.

In practical propagation studies, the path loss exponent n is determined experimentally from field measurement data because propagation conditions vary among urban, suburban, and rural environments. Estimating the path loss exponent is therefore essential for developing accurate propagation models and improving wireless network planning [23], [27], [28].

The Seybold Report
ISSN 1533-9211
DOI: 10.5281/zenodo.21867143

The path loss exponent (PLE), denoted by n, is one of the most important parameters of the Log-Distance Path Loss model because it characterizes the rate at which radio signals attenuate as they propagate through different environments.

Table 1: Typical Path Loss Exponent Values

Enveronment	Path Loss`Exponent (n)``
Free space	2.0
Urban cellular	2.7 - 3.5
Shawdow Urban	3.0 - 5.0
Indoor Line of Sight	1.6 - 1.8
Indoor Obstructed	4.0 – 6.0
Factory environment	2.0 – 3.0

The value of *n* depends on propagation conditions, including building density, vegetation, terrain morphology, and other obstacles that influence reflection, diffraction, and scattering. Consequently, the path loss exponent is typically estimated from field measurement data rather than assigned a fixed theoretical value [25]. The path loss exponent can be estimated as follows:

$$n - \frac{PL(dB) - PL(d_0)}{10\log_{10}\left(\frac{d}{d_0}\right)} \quad (7)$$

3. RESULT AND DISCUSSION

This section presents the characteristics of the radio wave propagation environments, the measurement results, and a statistical analysis of the received signal power attenuation along the propagation paths. It also discusses the estimation of the path loss exponent, the analysis of the average path loss, and a comparative evaluation of propagation losses across the three measurement environments. The detailed results and corresponding analyses are presented in the following subsections.

Overview of Radio Wave Environments

This subsection provides an overview of the three radio wave propagation environments selected for the field measurement campaign. The urban measurement site is located along Merdeka Street in Lhokseumawe, as shown in Figs. 2(a) and 2(b). The suburban site is located in Gampong Beunot, Syamtalira Bayu District, as illustrated in Figs. 2(c) and 2(d), while the rural site is situated in Gang Payah Jaloh, Linepipa Street, Punteut, Lhokseumawe, as shown in Figs. 2(e) and 2(f).

These locations were selected to represent distinct propagation environments with different building densities, vegetation cover, and terrain characteristics, thereby enabling a comprehensive comparison of radio wave propagation behavior under diverse environmental conditions.

ISSN 1533-9211
DOI: 10.5281/zenodo.21867143

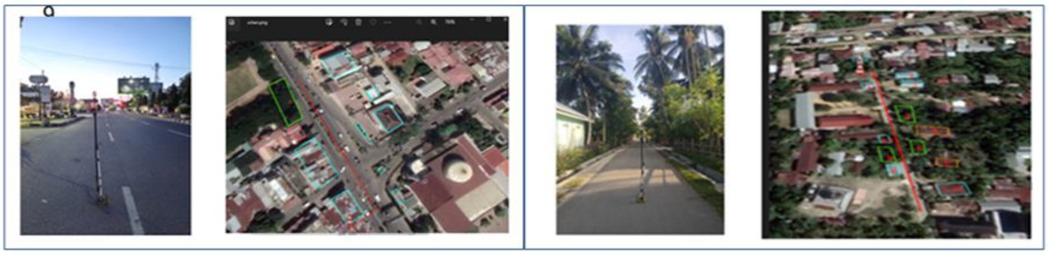

(a) (b) (c) (d)

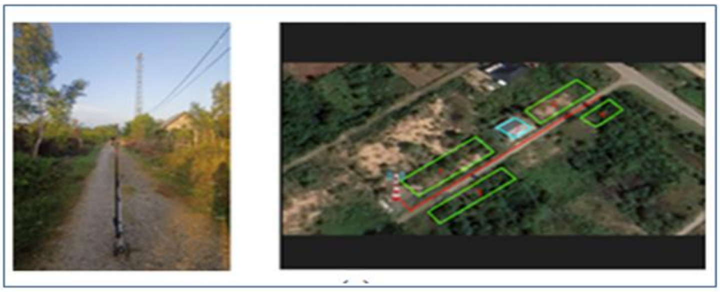

(e) (f)

Figure 2: Radio Wave Propagation Environments And Measurement Locations: (A) And (B) Urban Area On Merdeka Street, Lhokseumawe; (C) And (D) Suburban Area On Beunot Street, Syamtalira Bayu; And (E) And (F) Rural Area On Gang Payah Jaloh, Line Pipa Street, Punteut, Lhokseumawe

The urban environment, as illustrated in Fig. 2(a) and Fig. 2(b), is classified as a small-town area based on its population size, the availability and types of public facilities and infrastructure, and the regional development topology classification [17], [18]. Along the radio wave propagation path, the surrounding environment is predominantly characterized by permanent three-story reinforced concrete residential buildings, while a smaller proportion of the structures are roofed with galvanized steel sheets. Several trees are distributed throughout the area, providing urban green spaces. The roadway is approximately 16 m wide and consists of two traffic lanes separated by a central median. Based on field observations, the propagation path is dominated by reinforced concrete structures (72.44%), followed by trees (18.13%), iron structures (6.07%), and galvanized steel roofing materials (3.34%). The suburban environment, shown in Figs. 2(c) and 2(d), represents a newly developed residential area. Along the transmitter–receiver (T_x–R_x) propagation path, the surrounding structures consist predominantly of single-story houses with relatively low building density, resulting in large open spaces. Numerous trees, approximately 5–6 *m* in height, are distributed throughout the area. The road has an average width of approximately 4 m. Based on the field survey, the dominant materials along the propagation path are trees (47.78%), concrete (26.03%), wood (13.76%), and galvanized steel roofing (12.43%). The rural environment, illustrated in Figs. 2(e) and 2(f), is characterized by expansive open areas and sparsely distributed residential

ISSN 1533-9211

DOI: 10.5281/zenodo.21867143

buildings. Along the transmitter–receiver (T_x–R_x) propagation path, the houses are widely spaced and surrounded by dense vegetation. The trees in this area are generally 2–3 m in height. The road infrastructure consists of a paved road with an average width of approximately 3 *m*. Based on the field survey, the dominant materials along the propagation path are trees (89.99%), followed by wood (7.75%) and concrete structures (2.26%). A quantitative summary of the material composition for each propagation environment is presented in Table 2.

Table 2: Radio Wave Environment Materials

Environment	Material (%)				
	Trees	Concrete	Galvanized Steel Roof	Iron plate	Wood
Urban (small cyti)	18,13	72,44	3,34	6,07	0,0
Sub-Urban	47,78	26,03	12,43	0,0	13,76
Rural	89,99	2,26	0,0	0,0	7,75

Radio Transmitter Parameters for the Urban, Suburban, and Rural Propagation Environments

Table 3 summarizes the technical parameters of the base stations used in the field measurements across the urban, suburban, and rural propagation environments. Each measurement environment was served by a different cellular base station with distinct operating characteristics. The urban environment was served by Cell Id 21, operating at a carrier frequency of 1870 *MHz* with a transmit power of 24 *dBm* and a base station antenna height of 36 *m*. The suburban environment was served by Cell Id 23, operating at the same carrier frequency with a transmit power of 30 *dBm* and an antenna height of 41 *m*.

Similarly, the rural environment was served by Cell Id 11, operating at the same carrier frequency with a transmit power of 30 *dBm* and a base station antenna height of 42 *m*. These parameters represent the actual operating conditions of the cellular network during the measurement campaign and provide the basis for the subsequent path loss analysis.

Table 3: Technical Parameters of the Base Stations in Urban, Suburban, and Rural Environments

Environment	Cell id	Power Transmit (*dBm*)	Frequency (*MHz*)	Height Antenna under ground (*m*)
urban	21	24	1870	36
Suburban	23	30	1870	41
rural	11	30	1870	42

Signal Strength Measurement

The radio signal strength along the propagation path was measured using a mobile receiver equipped with the Network Cell Info Lite application. The application was used to monitor and record the Reference Signal Received Power (RSRP) at each measurement point following the measurement procedure illustrated in Fig. 1. RSRP was selected as the primary measurement parameter because it represents the average received power of LTE reference signals and is widely recognized as a reliable indicator for evaluating radio propagation characteristics and cellular network coverage. A total of 736 measurement samples were collected in each

ISSN 1533-9211

DOI: 10.5281/zenodo.21867143

propagation environment, namely urban, suburban, and rural. Measurements were conducted continuously along the transmitter–receiver (T_x–R_x) propagation path while maintaining a constant receiver height and following the predefined measurement route. The recorded RSRP data were subsequently converted into the received power level P_r using (3)–(5). The calculated received power values were then analyzed and plotted as propagation curves for the urban, suburban, and rural environments, as shown in Figs. 3(a), 3(b), and 3(c), respectivel

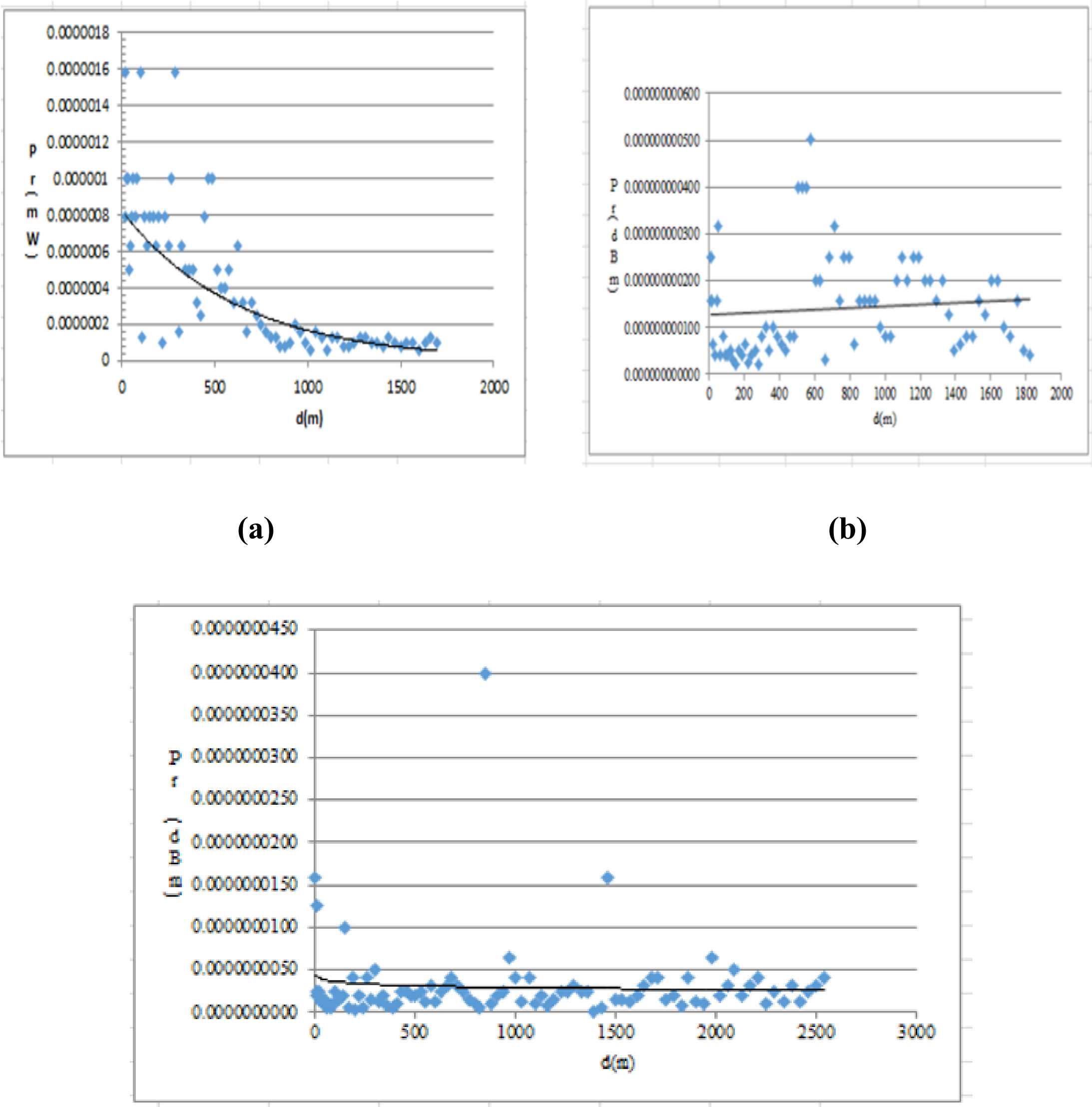

(a) (b)

(c)

Figure 3: Measured received power along the transmitter–receiver (T_x–R_x) propagation path in (a) urban, (b) suburban, and (c) rural environments

The Seybold Report
ISSN 1533-9211
DOI: 10.5281/zenodo.21867143

The received power characteristics shown in Fig. 3 are strongly influenced by the material composition of the propagation environments summarized in Table 2. The proportions of concrete, vegetation, wood, galvanized steel roofing, and iron distributed along the transmitter–receiver (T_x–R_x) propagation path determine the dominant radio propagation mechanisms, including reflection, diffraction, scattering, penetration, and absorption. Because these mechanisms depend on the physical properties and spatial distribution of surrounding objects, each propagation environment exhibits a distinct received power profile.

As shown in Fig. 3(a), the urban environment exhibits a rapid decrease in received power with increasing propagation distance, accompanied by pronounced short-distance fluctuations. According to Table 2, reinforced concrete structures constitute the dominant material 72.44%, whereas vegetation accounts for only 18.13% of the surrounding environment. Reinforced concrete buildings have relatively high dielectric constants and large reflective surfaces, resulting in strong specular reflections and the formation of multiple propagation paths. As the radio signal propagates through this environment, it repeatedly interacts with building facades, commercial buildings, and roadside structures, leading to multiple reflections, diffraction around building edges, and penetration losses. These propagation mechanisms produce severe multipath fading, which explains the rapid fluctuations observed in the received power curve. Although reflected signals may combine constructively at certain receiver locations, destructive interference predominates over longer propagation distances, resulting in a continuous decline in the average received power.

The suburban environment, illustrated in Fig. 3(b), exhibits a smoother variation in received power than the urban environment. As summarized in Table 2, the surrounding materials are more evenly distributed, consisting of 47.78% vegetation, 26.03% concrete, 13.76% wood, and 12.43% galvanized steel roofing. This balanced material composition creates a propagation channel with fewer dense building obstructions and larger open spaces between residential buildings. Consequently, the line-of-sight (LOS) component remains dominant over much of the measurement route, while the lower concentration of concrete structures reduces severe multipath reflections. Instead, vegetation becomes the primary source of attenuation, introducing moderate scattering and absorption rather than strong reflections. As a result, the received power decreases more gradually with increasing propagation distance and exhibits smaller fluctuations than those observed in the urban environment, indicating a more stable propagation channel.

The rural environment, shown in Fig. 3(c), exhibits propagation characteristics that differ markedly from those of the urban and suburban environments. According to Table 2, vegetation accounts for approximately 89.99% of the propagation path, whereas concrete structures constitute only 2.26%. The limited number of buildings substantially reduces reflection-induced multipath propagation; however, dense vegetation becomes the dominant source of signal attenuation.

As radio waves propagate through trees, they undergo absorption by leaves and branches, scattering caused by the irregular geometry of the vegetation, and partial depolarization of the electromagnetic field. Consequently, although the rural environment contains relatively few

ISSN 1533-9211
DOI: 10.5281/zenodo.21867143

artificial obstacles, the radio signal continuously loses energy while propagating through vegetation. This explains why the received power remains relatively low throughout the measurement route despite the presence of open spaces and sparsely distributed residential buildings. A comparison of the three propagation environments demonstrates that the received power characteristics shown in Fig. 3 closely correspond to the material compositions summarized in Table 2 The urban environment, dominated by reinforced concrete structures, experiences severe multipath propagation and significant penetration losses. The suburban environment, characterized by a balanced distribution of vegetation and buildings, exhibits moderate attenuation with relatively stable received power variations. In contrast, the rural environment is dominated by vegetation, where absorption and diffuse scattering are the primary mechanisms responsible for signal attenuation. These observations indicate that the composition and spatial distribution of surrounding materials have a direct influence on large-scale radio wave propagation and should therefore be considered when estimating propagation parameters and developing environment-specific path loss models.

Overall, the strong agreement between the measured received power profiles shown in Fig. 3 and the environmental characteristics summarized in Table 2 confirms that material composition is one of the primary factors governing radio signal attenuation. The measurement results further demonstrate that propagation behavior cannot be explained solely by propagation distance; rather, it is strongly influenced by the type, density, and spatial distribution of obstacles along the propagation path. Therefore, accurate wireless network planning requires propagation models that account for the dominant environmental characteristics of the deployment environment.

Pathloss Exponent

The propagation constant, commonly expressed as the path loss exponent (n), characterizes the rate at which radio signal attenuation increases with propagation distance. The path loss exponent reflects the propagation characteristics of a given environment and quantifies how rapidly path loss increases as the transmitter–receiver (T_x–R_x) separation distance grows. In this study, the path loss exponent for the three investigated propagation environments was estimated using (5) based on the measured received power as a function of propagation distance under different environmental conditions, following the measurement procedure illustrated in Fig. 1. The estimated path loss exponent values for the urban, suburban, and rural environments are summarized in Table 4.

Table 4: Results of the Path Loss Exponent Calculation

Radio wave Environment	Number of measurement sample (N)	Exponent pathloss (n)
Urban	959	3.1
Sub-urban	947	3.4
Rural	953	3.7

As summarized in Tables 2 and 3, the path loss exponent increases from 3.1 in the urban environment to 3.7 in the rural environment. This trend indicates that the material composition of the propagation environment has a significant influence on radio wave attenuation. The urban environment, dominated by reinforced concrete structures (72.44%), exhibits the lowest

The Seybold REPORT
ISSN 1533-9211
DOI: 10.5281/zenodo.21867143

path loss exponent because strong multipath propagation partially compensates for propagation loss through constructive signal components. In contrast, the rural environment, where vegetation accounts for 89.99% of the propagation path, exhibits the highest path loss exponent due to the increased absorption and scattering caused by dense vegetation. The suburban environment exhibits intermediate propagation characteristics, reflecting its balanced distribution of vegetation and built structures.

Comparison of Pathloss Characteristic

The path loss was calculated using (3) based on the received power measurements collected along the transmitter–receiver (T_x–R_x) propagation path for the three propagation environments illustrated in Figs. 2(a)–2(f). The received power measurements are presented in Figs. 3(a)–3(c), whereas the resulting path loss characteristics are shown in Figs. 4(a)–4(c). Figures 4(a)–4(c) illustrate the variation in the average path loss as a function of the transmitter–receiver (T_x–R_x) separation distance for the urban, suburban, and rural propagation environments. In all three environments, the average path loss increases with increasing propagation distance, reflecting the progressive attenuation of the radio signal as it propagates through the environment.

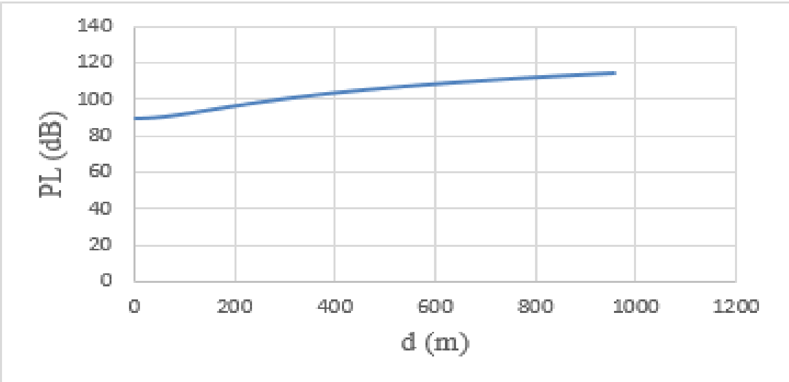

(a)

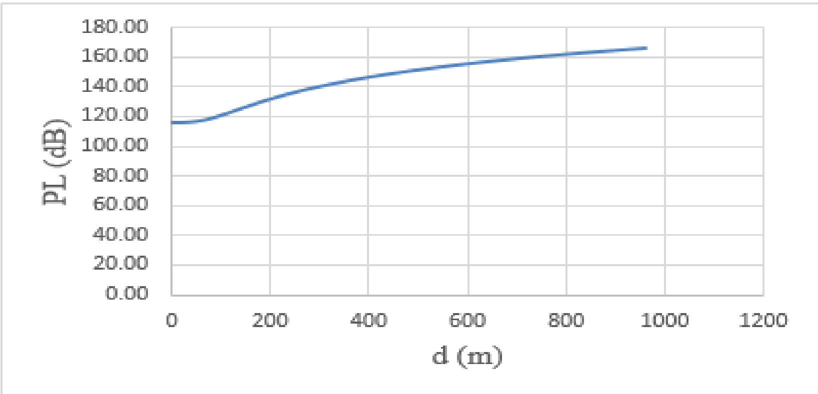

(b)

The Seybold REPORT
ISSN 1533-9211
DOI: 10.5281/zenodo.21867143

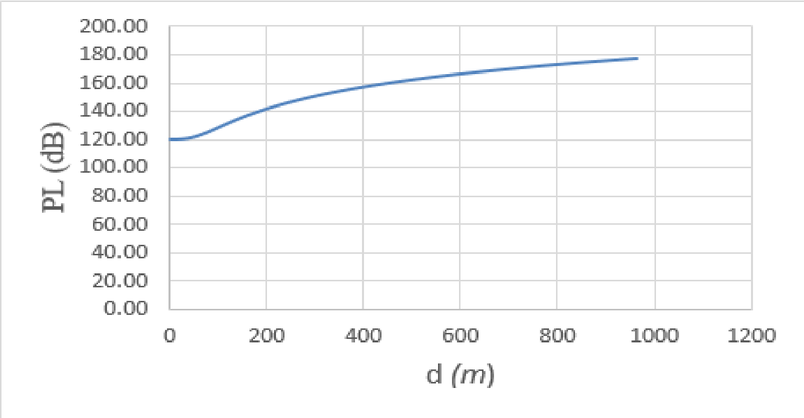

(c)

Figure 4: Path Loss Characteristics in (A) Urban, (B) Suburban, and (C) Rural Environments

Among the three propagation environments, the urban area exhibits the highest path loss because of the high density of buildings and other man-made structures, which increase signal attenuation through reflection, diffraction, and scattering. The suburban environment experiences moderate path loss due to the combined effects of buildings and vegetation. In contrast, the rural environment exhibits the lowest path loss because of its relatively open terrain and the limited presence of propagation obstacles.

These findings confirm that the characteristics of the propagation environment have a significant influence on radio wave attenuation and the resulting path loss.

As the propagation distance increases, the differences in path loss among the three environments become more pronounced. At the same transmitter–receiver separation distance, the urban environment consistently exhibits greater path loss than the suburban and rural environments, indicating that signal attenuation is strongly affected by the density of surrounding obstacles.

Conversely, the rural environment maintains the lowest path loss throughout the entire measurement range because its relatively unobstructed terrain provides more favorable propagation conditions.

Comparison Average Pathloss

Based on the measurement data presented in Fig. 3, the average path loss for the three propagation environments was calculated using (5). The resulting average path loss values are summarized in Table 5. The results indicate that the average path loss increases progressively from 103.897 *dB* in the urban environment to 146.791 *dB* in the suburban environment, reaching the highest value of 155.589 *dB* in the rural environment.

The Seybold Report
ISSN 1533-9211
DOI: 10.5281/zenodo.21867143

Table 5: Average Path Loss and Environmental Material Composition in Urban, Suburban, and Rural Environments

Environment	Material (%)					$\overline{PL}$ (dB)
	Trees	concrete	Galvanized Steel Roof	Iron plate	Wood	
Urban (small cyti)	18,13	72,44	3,34	6,07	0,0	103.897
Sub-Urban	47,78	26,03	12,43	0,0	13,76	146.791
Rural	89,99	2,26	0,0	0,0	7,75	155.589

This trend indicates that the rural measurement route experienced the greatest signal attenuation, whereas the urban route exhibited the lowest attenuation among the three propagation environments. The differences in the average path loss indicate that environmental characteristics, including terrain profile, vegetation density, and the distribution of obstacles along the propagation path, have a significant influence on radio wave propagation. Although urban environments are generally characterized by a high density of buildings, which typically increase signal attenuation through reflection, diffraction, and scattering, the measurement results in this study show that the rural environment exhibited the highest path loss. This finding suggests that propagation path geometry, line-of-sight conditions between the transmitting and receiving antennas, terrain irregularities, and dense vegetation along the propagation path—particularly in the suburban and rural environments have a greater influence on signal attenuation than building density alone.

These results demonstrate that path loss is strongly site-dependent and is governed by the combined effects of the local propagation environment rather than by a single environmental factor. The higher path loss observed in the rural environment further indicates that dense vegetation and local terrain features were the dominant factors contributing to the increased attenuation of the received signal under the measured propagation conditions.

4. CONCLUSIONS

This study investigated radio wave propagation characteristics in urban, suburban, and rural environments through field measurements conducted along the propagation path between the transmitter (T_x) and receiver (R_x). The received power measurements were used to calculate the path loss using the Log-Distance Path Loss model. The results demonstrate that path loss increases with transmitter–receiver separation distance across all propagation environments, confirming the progressive attenuation of radio signals during propagation. The average path loss values obtained from the measurements were 103.897 *dB,* 146.791 *dB*, and 155.589 *dB* for the urban, suburban, and rural environments, respectively. The findings confirm that the propagation environment has a significant influence on radio wave attenuation and path loss characteristics. The observed differences indicate that, in addition to building density, site-specific factors such as vegetation density, terrain profile, propagation path geometry, line-of-sight conditions, and the distribution of obstacles along the propagation path play important roles in determining signal attenuation. These results also demonstrate that propagation characteristics are highly site-dependent and cannot be accurately represented by a single environmental parameter.

DOI: 10.5281/zenodo.21867143

Therefore, field measurements remain essential for accurately characterizing radio wave propagation under practical wireless communication conditions and for developing reliable propagation models for network planning and performance evaluation. Future work will focus on validating the measurement results against established empirical propagation models and extending the analysis to additional frequency bands and fifth-generation (5G) wireless communication systems.

Acknowledgement

The author would like to express his sincere gratitude to his Head of the Research and Community Service Center, Dr. Amir Fauzi, for his invaluable guidance, continuous support, and insightful advice throughout this research. The author also extends his sincere appreciation to the members of the Radio Wave Propagation and Modelling (RWPM) Research Group, Politeknik Negeri Lhokseumawe, Aceh, Indonesia, for their outstanding collaboration in the data collection and analysis processes. Their expertise, dedication, and valuable contributions have been instrumental to the successful completion of this study.

References

1) N. Blaunstein, *Radio Propagation in Cellular Networks*. Norwood, MA, USA: Artech House, 2000.

2) V. K. Garg, *Wireless Communications and Networking*. Burlington, MA, USA: Morgan Kaufmann, 2007, Ch. 3: "Radio Propagation and Propagation Path-Loss Models."

3) A. Goldsmith, *Wireless Communications*. Cambridge, U.K.: Cambridge University Press, 2005, Ch. 2: "Path Loss and Shadowing."

4) C. Haslett, *Essentials of Radio Wave Propagation*. Cambridge, U.K.: Cambridge University Press, 2008.

5) J. A. Richards, *Radio Wave Propagation: An Introduction for the Non-Specialist*. Berlin, Germany: Springer, 2008.

6) S. Ojo, A. Imoize, and D. Alienyi, "Radial basis function neural network path loss prediction model for LTE networks in multitransmitter signal propagation environments," *International Journal of Communication Systems*, vol. 34, no. 3, 2021.

7) F. Wen *et al*., "Measurement and Modeling of LTE-Railway Channels in High-Speed Railway Environment," *Radio Science*, vol. 55, no. 3, 2020.

8) J. D. Gadze, K. A. Agyekum, S. J. Nuagah, and E. A. Affum, "Improved propagation models for LTE path loss prediction in urban and suburban Ghana," 2020.

9) A. de Souza *et al*., "On the application of generalized linear mixed models for predicting path loss in LTE networks," *EURASIP Journal on Advances in Signal Processing*, 2022.

10) Z. S. Kareem, G. A. Aramice, and A. H. Miry, "Empirical Analysis of Path Loss and Distance Estimation in Wireless Networks," *Journal of Electrical Systems and Automation (JESA)*, 2025.

11) T. S. Rappaport, Y. Xing, G. R. MacCartney Jr., A. F. Molisch, E. Mellios, and J. Zhang, "Overview of Millimeter Wave Communications for Fifth-Generation (5G) Wireless Networks—With a Focus on Propagation Models," *IEEE Transactions on Antennas and Propagation*, vol. 65, no. 12, pp. 6213–6230. *(Masih menjadi referensi utama untuk propagation modeling meskipun terbit sebelum 2020.)*

12) A. F. Molisch, *Wireless Communications*, 3rd ed. Hoboken, NJ, USA: Wiley, 2023.

13) A. F. Molisch, *Wireless Communications*, 3rd ed. Hoboken, NJ, USA: Wiley, 2023.

ISSN 1533-9211

DOI: 10.5281/zenodo.21867143

14) 3GPP TS 36.214, Evolved Universal Terrestrial Radio Access (E-UTRA); Physical Layer; Measurements, Release 17, 3GPP, 2022.

15) H. Holma, A. Toskala, T. Nakamura, *et al.*, LTE to 5G Evolution: The End of LTE as We Know It, 2nd ed. Wiley, 2020.

16) S. M. A. Al-Samman, T. A. Rahman, M. H. Azmi, *et al.*, "Outdoor Propagation Measurements and Path Loss Models for Wireless Communication Networks: A Review," *IEEE Access*, vol. 9, pp. 121649–121665, 2021.

17) M. A. Hossain, M. R. Islam, and M. T. Islam, "Performance Evaluation of LTE Networks Based on Drive Test Measurements in Urban and Suburban Environments," *IEEE Access*, vo10, pp. 67580–67595, 2022.

18) A. F. Molisch, *Wireless Communications: From Fundamentals to Beyond 5G*, 3rd ed. Hoboken, NJ, USA: Wiley-IEEE Press, 2023.

19) 3GPP TS 36.214, *Evolved Universal Terrestrial Radio Access (E-UTRA); Physical Layer Measurements*, Release 17, 3GPP, 2022.'

20) T. S. Rappaport, *Wireless Communications: Principles and Practice*, 2nd ed. Upper Saddle River, NJ, USA: Prentice Hall, 2002.

21) ITU-R Recommendation P.1411-11, *Propagation Data and Prediction Methods for the Planning of Short-Range Outdoor Radiocommunication Systems*, International Telecommunication Union (ITU), Geneva, Switzerland, 2023.

22) H. Holma and A. Toskala, *LTE to 5G Evolution: The End of LTE as We Know It*, 2nd ed. Hoboken, NJ, USA: Wiley, 2020.

23) S. M. A. Al-Samman, T. A. Rahman, M. H. Azmi, *et al*., "A Survey of Propagation Models for Wireless Communication Networks," *IEEE Access*, vol. 9, pp. 120482–120506, 2021.

24) M. A. Hossain, M. R. Islam, and M. T. Islam, "Performance Evaluation of LTE Networks Based on Drive Test Measurements," *IEEE Access*, vol. 10, pp. 67580–67595, 2022.

25) A. F. Molisch, *Wireless Communications*, 3rd ed. Hoboken, NJ, USA: Wiley, 2023.

26) T. S. Rappaport, *Wireless Communications: Principles and Practice*, 2nd ed. Upper Saddle River, NJ, USA: Prentice Hall, 2002.

27) T. S. Rappaport *et al*., "Overview of Millimeter Wave Communications for Fifth-Generation Wireless Networks," *IEEE Transactions on Antennas and Propagation*, vol. 65, no. 12, pp. 6213–6230, 2017.

28) S. M. A. Al-Samman, T. A. Rahman, M. H. Azmi, *et al*., "A Survey of Propagation Models for 4G and 5G Wireless Networks," *IEEE Access*, vol. 9, pp. 120482–120506, 2021.

29) H. Holma and A. Toskala, *LTE to 5G Evolution: The End of LTE as We Know It*, 2nd ed. Wiley, 2020.

30) D. C. Montgomery, E. A. Peck, and G. G. Vining, *Introduction to Linear Regression Analysis*, 6th ed. Wiley, 2021.

31) T. S. Rappaport, *Wireless Communications: Principles and Practice*, 2nd ed. Upper Saddle River, NJ, USA: Prentice Hall, 2002.

32) T. S. Rappaport *et al*., "Overview of Millimeter Wave Communications for Fifth-Generation Wireless Networks," *IEEE Transactions on Antennas and Propagation*, vol. 65, no. 12, pp. 6213–6230, 2017.

33) A. Goldsmith, *Wireless Communications*. Cambridge University Press.